Published in Optics Express 14, issue 7, 2969-2978, 2006
which should be used for any reference to this work

Tuning the resonance of a photonic crystal microcavity with an AFM probe

Iwan Märki, Martin Salt[1] and Hans Peter Herzig

Institute of Microtechnology, University of Neuchâtel, Rue A.-L. Breguet 2, CH-2000 Neuchâtel, Switzerland
[1] Present address: Heptagon Oy, Moosstrasse 2, CH-8803 Rüschlikon, Switzerland.
iwan.maerki@unine.ch

Abstract: We present theoretical and experimental results on switching and tuning of a two-dimensional photonic crystal resonant microcavity by means of a silicon AFM tip, probing the highly localized optical field in the vicinity of the cavity. On-off switching and modulation of the transmission signal in the kHz range is achieved by bringing an AFM tip onto the center of the microcavity, inducing a damping effect on the transmission resonance. Tuning of the resonant wavelength in the order of several nanometers becomes possible by inserting the AFM tip into one of the holes of the Bragg mirror forming the microcavity in the propagation direction.

References and Links

1. E. Yablonovitch, "Photonic band-gap structures", J. Opt. Soc. Am. B **10**, 283-295, (1993).
2. J. D. Joannopoulos, R. D. Maede, J. N. Winn, *Photonic Crystals*, Princeton University Press, Princeton, (1995).
3. S. G. Johnson, S. Fan, P. R. Villeneuve, J. D. Joannopoulos, L. A. Kolodziejski, "Guided modes in photonic-crystal slabs," Phys. Rev. B **60**, 5751-5780, (1999).
4. A. Mekis, J. C. Chen, I. Kurland, S. Fan, P. Villeneuve, J. D. Joannopoulos, "High Transmission through Sharp Bends in Photonic Crystal Waveguides," Phys. Rev. Lett. **77**, 3787-3790 (1996).
5. M. Notomi, A. Shinya, S. Mitsugi, E. Kuarmochi, H-Y. Ryu ,"Waveguides, resonators and their coupled elements in photonic crystal slabs," Opt. Express **12**, 1554-1561 (2004).
6. I. Märki, M. Salt and H. P. Herzig, "Practical and theoretical modal analysis of photonic crystal waveguides," J. Appl. Phys. **95**, 7-11, (2004).
7. S. Fan, P. R. Villeneuve, J. D. Joannopoulos, "Channel drop filters in photonic crystals," Opt. Express **3**, 4-11, (1998).
8. S. Noda, A. Chutinan, M. Imada, "Trapping and emission of photons by a single defect in a photonic bandgap structure," Nature **407**, 608-610, (2000).
9. M. Lončar, T. Yoshie, A. Scherer, "Low threshold photonic crystal laser," Appl. Phys. Lett. **81**, 2680-2682 (2002).
10. J. Vučković, M. Lončar, H. Mabuchi, A. Scherer, "Design of photonic crystal microcavities for cavity QED," Phys. Tev. E **65**, 016608, (2001).
11. K. Srinivasan, O. Painter, "Momentum space design of high-Q photonic crystal optical cavities," Opt. Express **10**, 670-684, (2002).
12. Y. Akahane, T. Asano, B-S Song, S. Noda, "Fine-tuned high-Q photonic-crystal nanocavity," Opt. Express 13, 1202-1214, (2005).
13. A. F. Koenderink, M. Kafesaki, B. C. Buchler, V. Sandoghdar, "Controlling the Resonance of Photonic Crystal Microcavity by a Near-Field Probe," Phys. Rev. Lett. **95**, 153904 (2005).
14. Y. Akahana, T. Asano, B-S Song, S. Noda, "High-Q photonic nanocavity in two-dimensional photonic crystal," Nature **425**, 944-947, (2003).
15. Ph. Lalanne, J. P. Hugonin, "Bloch-wave engineering for high Q's, small V's microcavities," IEEE J. Quantum Electron. **39**, 1430-1438, (2003).
16. Ph. Lalanne, S. Mias, J. P. Hugonin, "Two physical mechanisms for boosting the quality factor to cavity volume ratio of photonic crystal microcavities," Opt. Express **12**, 458-466, (2004).
17. C. C. Cheng and A. Scherer, "Fabrication of photonic band-gap crystals," J. Vac. Sci. Technol. B **13**, 2696, (1995).

18. T. Weiland, "A discretization method for the solution of Maxwell's equations for six-component fields," Electron. Commun. **31**, 116-120, 1977.
19. E. A. Camargo, H. M. H. Chong and R. M. De La Rue, "2D Photonic crystal thermo-optic switch based on AlGaAs/GaAs epitaxial structure," Opt. Express **12**, 588-592, (2004).
20. B. Wil, R. Ferrini, R. Houdré, M. Mulot, S. Anand, C. J. M. Smith, "Temperature tuning of the optical properties of planar photonic crystal microcavities," Appl. Phys. Lett. **84**, 846-848, (2004).
21. D. M. Pustai, A. Sharkawy, S. Shi, D. W. Prather, "Tunable photonic crystal microcavities," Appl. Opitcs **41**, 5574-5579, (2002).
22. Ch. Schuller, F. Klopf, J. P. Reithmaier, M. Kamp, and A. Forchel, "Tunable photonic crystals fabricated in III-V semiconductor slab waveguides using infiltrated liquid crystals," Appl. Phys. Lett. **82**, 2767-2769, (2003).
23. S. M. Weiss, H. Ouyang, J Zhang, Ph. M. Fauchet, "Electrical and thermal modulation of silicon photonic bandgap microcavities containing liquid crystals," Opt. Express **13**, 1090-1097, (2005).
24. D. Erickson, T. Rockwood, T. Emery, A. Scherer, D. Psaltis, "Nanofluidic tuning of photonic crystal circuits", Opt. Lett. **31**, 59-61, (2006).
25. A. Sharkawy, S. Shi, D. W. Prather, "Electro-optical switching using coupled photonic crystal waveguides", Opt. Express **10**, 1048-1059, (2002).
26. S. W. Leaonard H. M. van Driel, J. Schilling and R. B. Wehrsporn, "Ultrafast band-edge tuning of a two-dimensional silicon photonic crystal via free-carrier injection," Phys. Rev. B **66**, 161102, (2002).
27. F. Raineri, C. Cojocaru, R. Rai, P. Monnier, A. Levenson, C. Seassal, X. Letartre, P. Viktorovitch, "Tuning a two-dimensional photonic crystal resonance via optical carrier injection," Opt. Lett. **30**, 64-66, (2005).
28. P. E. Barclay, K. Srinivasan, O. Painter, "Nonlinear response of silicon photonic crystal microresonators excited via an integrated waveguide and fiber taper," Opt. Express **13**, 801-820, (2005).
29. I. Märki, M. Salt, H. P. Herzig, R. Stanley, L. El Melhaoui, P. Lyan, J. M. Fedeli, "Optically tunable microcavity in a planar photonic crystal silicon waveguide buried in oxide," Opt. Lett. **31**, 011604, (2006).
30. W. Park, J.-B. Lee, "Mechanically tunable photonic crystal structure," App. Phys. Lett. **85**, 4845-4547, (2004).
31. S. Iwamoto, S. Ishida, Y. Arakawa, M. Tokushima, A. Gomyo, H. Yamada, A. Higo, H. Toshiyoshi, H. Fujita, "Observation of micromechanically controlled tuning of photonic line-defect waveguide," App. Phys. Lett. **88**, 011104 (2006).
32. T. Takahata, K. Hoshino, K. Matsumoto, I. Shimoyama, "Photonic crystal tuned by cantilever", 18th IEEE International Conference on Micro Electro Mechanical Systems, Miami, Florida, USA, January 30 - February 3, 2005.

1. Introduction

Photonic crystals are periodic structures with lattice dimensions of the order of the wavelength of light and they offer the ability to control light propagation on a wavelength scale [1-3]. One of the most promising realizations of photonic crystals is the well known two-dimensional planar photonic crystal slab, which confines the light by means of a photonic band gap in-plane and through index guiding in the vertical direction. These structures provide the possibility of creating miniaturized photonic components for integrated optical circuits [4-6]. An area of great interest in the process of realizing photonic integration is the use of photonic microcavities in two-dimensional photonic crystal waveguides for particular waveguide functions, such as small filters, microlasers, multiplexers, optical switches and high-resolution sensors [7-9]. Photonic microcavities can confine light in very small volumes ($\sim\lambda^3$) and exhibit high spectral resolution. Therefore, they could be key components for a variety of applications. The cavity Q factor per modal volume, Q/V, is one of the characteristic quantities that determine the strength of various interactions within the cavity. In recent years the optimization of such microcavities with increased factors has been the subject of intense research [10-12].

One of the difficulties associated with such photonic crystal cavity structures is to match their resonance frequency with those of interest in a given application. This is especially a concern since already small fabrication induced variations and irregularities cause a change in the optical properties of the cavity structure. The ability to tune or modulate the optical properties of such devices increases their functionality and opens up new possibilities for a variety of applications for integrated optics.

In this paper, we present theoretical and first experimental results on tuning and switching the optical properties of a photonic crystal microcavity by means of a mechanical actuation

method. A Silicon AFM tip is used to probe the localized optical field in the vicinity of the cavity achieving damping and tuning of the transmission resonance as theoretically predicted by A.F. Koenderink et al. in a similar configuration [13]. The theoretical and experimental results suggest a stand-alone MEMS solution to create a chip-based device with switching and tuning functionalities.

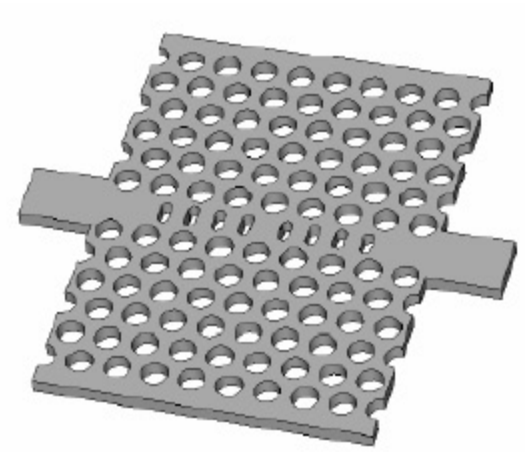

Fig. 1. In-plane photonic crystal microcavity membrane consisting of a triangular array of cylindrical holes (period 520 nm and hole radius 182 nm) in a thin Si membrane layer (thickness 205 nm) surrounded by air.

2. Design

The design geometry of the in-plane resonant cavity we have chosen is shown in Fig. 1. The photonic crystal consists of a triangular array of cylindrical holes (period 520 nm and hole radius 182 nm) in a thin Si layer (thickness 205 nm) for lateral light confinement. The in-plane resonant cavity is formed by two identical one-dimensional Bragg reflectors embedded in the photonic crystal waveguide and has a length of 400 nm (distance between the two Bragg reflectors) confining the light to an effective volume of approximately $200 \times 500 \times 500$ nm at resonant wavelength. The design parameters of the Bragg reflectors (hole width 350 nm, hole length 150 nm, Bragg period 380 nm) are different to those of the rest of the photonic crystal. This increases the design options for the cavity and allows more efficient coupling into and out off the cavity than the surrounding triangular photonic crystal arrangement. The entire structure is surrounded by air and is thus a membrane.

The cavity structure is designed so as to obtain a highly localized field inside the cavity and high in-plane transmission for a narrow frequency band. In order to achieve a high Q factor and high in-plane transmission, the radiation losses (i.e. the modal mismatch at the interface between the photonic crystal waveguide and the cavity structure) need to be minimized by engineering the hole dimensions and positions of the Bragg reflectors during the design process. Several methods have been suggested for optimizing the performance of photonic crystal microcavities, including tapering [14], Bloch-wave engineering [15] or radiation loss recycling [16]. All these methods require a very high accuracy and quality for the fabrication. For example, Noda et. al. have realized high-Q photonic crystal microcavities with Q factors up to 100,000 by optimizing the position of the air holes at both edges of the cavity [12]. Limited by the fabrication tolerances, we have kept our design as simple as possible while accepting lower performance for the cavity. Thus, the holes of the one-dimensional Bragg reflectors are all equally spaced and have the same dimensions (350 nm $\times$ 150 nm).

The device has been fabricated in-house at the IMT-Samlab (University of Neuchâtel) using e-beam lithography [17]. The microcavity structure is written into a PMMA layer and

then RIE and DRIE is used to transfer the structure from the PMMA layer into the Silicon. Lastly, buffered hydrofluoric acid vapour (BHF) etching removes the silicon dioxide layer underneath the Silicon slab forming a free-standing silicon membrane.

To measure the sample a butt-coupling setup was used. By means of a tapered fiber, TE-polarized light (in-plane polarization) from a tunable laser source (1440 nm to 1590 nm) is injected into a 10 μm-wide silicon layer (thickness t = 205 nm). A lateral taper is used to reduce the waveguide width to the 0.5 μm width of the photonic crystal waveguide. For a narrow frequency band the light propagating in the photonic crystal waveguide couples into the resonant cavity, where it is highly localized and then transmitted. Using a second, identical taper the transmitted light is then guided to the exit of the device, where it is collected by a microscope objective and focused onto an InGaAs detector.

3. Passive transmission measurements

We have fabricated and measured several samples with the designed microcavities, exhibiting Q-factors between 300 and 750 for resonant wavelengths between 1.47 and 1.52 μm. In Fig. 2(a) we present one of the measured transmission spectra of the photonic crystal microcavity. For this sample, the measured transmission spectrum exhibits a resonance peak at the wavelength of 1.47 μm and a Q-factor of approximately 750. The dominant periodic Fabry-Pérot interference pattern contained within the measured spectrum corresponds to the total length of the waveguide system (approximately 2 mm) and is due to the Fresnel reflections at the smooth waveguide end-facets. Our three dimensional simulations have shown that about 38% of the light is reflected at the silicon/air interface of each end-facet.

The calculated transmission spectrum using a three dimensional finite integral time domain technique [18] is shown in Fig. 2(b). In the inset the field distribution (magnetic field perpendicular to the photonic crystal membrane) at the transmission resonance peak illustrates the strong light confinement within the cavity. The measured Q-factor is about half of the predicted value by the calculation. Such differences are due to variations between the fabricated structure and the ideal simulated structure. Small defects, like variations in the hole dimensions or sidewall roughness, also induce higher losses, which cause a reduction in transmission and in the quality factor. Further improvements to the quality factor of the resonant cavity can be achieved by optimizing the design of the photonic crystal waveguide and the reflectors forming the microcavity.

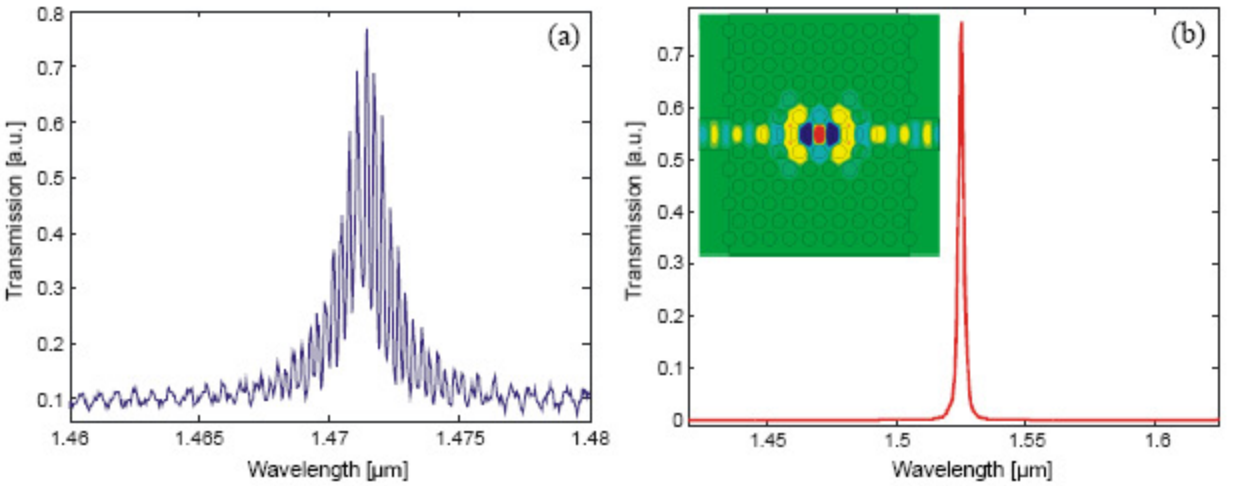

Fig. 2. (a) Measured transmission spectrum of a photonic crystal cavity structure in a membrane surrounded by air with a Q factor of approximately 750. The characteristic Fabry-Perot interference pattern at resonance is mainly due to end-facet reflections corresponding to a total waveguide length of 2 mm where as off resonance the interference pattern (2 times longer peak separation) is mainly due to end-facet to cavity reflections corresponding to an optical path of 1 mm (cavity structure is situated in the middle of the waveguide). (b) Calculated transmission spectrum of the ideal photonic crystal cavity structure with a Q factor in the order of 1500. The inset shows the calculated field distribution (magnetic field perpendicular to the photonic crystal membrane) at the resonance wavelength.

4. Tuning and switching

The highly localized field within the resonant microcavity is very sensitive to any perturbation. By a local change in the structure or the environment of the cavity one can influence the optical transmission properties. Ideally, such a change should be reversible so that we can realize an active, tunable device on a very small scale. Various ways to tune or switch photonic crystal devices have been demonstrated recently. One of the most common ways is temperature tuning induced by the temperature dependence of the refractive index of the material [19,20]. However, with this method it is difficult to locally restrict the tuning effect on a chip. Both, theoretical [21] and experimental [22,23] work has demonstrated the possibility of infiltrating photonic structures with liquid crystals and achieve the desired modulation by electromagnetically rotating the director field of the liquid crystal or thermally inducing a phase transition in the liquid crystal. Tunable spectral filtering of a planar photonic crystal has been demonstrated by means of a nanofluidic delivery structure using fluids with different refractive indices [24]. Electro-optical switching has been presented using a PN junction to inject free charge carriers and induce electro-absorption [25]. Further, all-optical switching has been demonstrated by different groups [26-29] with time responses varying from ms to fs depending on the mechanism and materials used. First results on mechanically tunable photonic crystal structures point out their great potential for multifunctional integrated optical devices [30-32]. One of the objectives of today's on-going research is to increase the tuning and switching performances and to achieve applicability for tuneable photonic crystal devices. Here, we present theoretical and experimental results on tuning and switching the optical properties of a photonic crystal microcavity based on the mechanical perturbation of the optical field.

Because the photonic crystal structure is a free-standing membrane, it allows direct access to the cavity and therefore direct mechanical intervention becomes possible. Our mechanical actuation method consists in bringing a silicon tip into the vicinity of the microcavity in order to induce a change in the optical environment. This can be achieved by introducing an AFM into the measurement setup and by probing the photonic crystal cavity region, as indicated in Fig. 3.

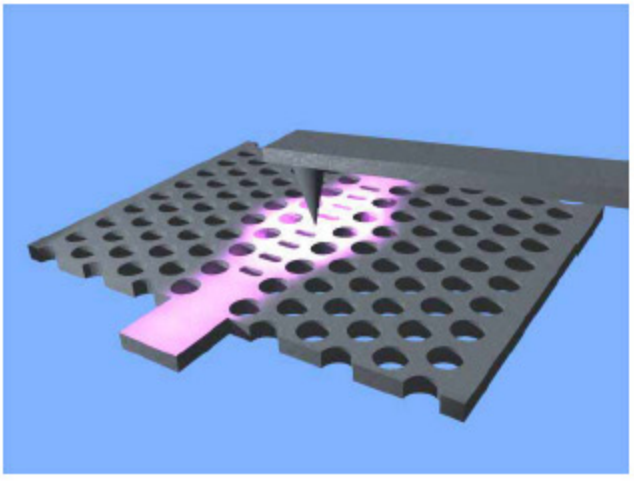

Fig. 3. Silicon AFM tip positioned above the cavity center perturbing the confined optical field in order to induce on-off switching.

In a first configuration, we bring an AFM tip onto the center of the cavity perturbing the optical field. As shown in the field distribution at the resonance wavelength in Fig. 2, the optical field is highly localized in the center of the cavity and therefore very sensitive to any changes in the environment. In Fig. 4(a) we show the simulated changes in the in-plane transmission properties of the microcavity when approaching the silicon tip to the surface of the membrane (three tip-surface distances) using the 3-D finite integral time domain technique. The tip used in the simulation is shaped like a polygon based pyramid and has a tip radius of curvature of 30 nm. The simulations predict that the closer the Silicon tip to the surface of the photonic structure the stronger is the damping effect on the transmission efficiency. Virtually complete damping of the transmitted signal can be achieved when the tip is positioned on the surface of the membrane. Thus, by moving this small silicon tip over a distance as small as 500 nm, on-off switching becomes possible. In the inset of Fig. 4(a), the absolute value of the calculated field distribution illustrates how a part of the optical field confined within the cavity is coupled into the probing silicon tip inducing damping in the transmission efficiency and reducing the Q factor of the cavity. Our simulations show that due to the presence of the probing tip approximately 15% of the light is coupled into the tip, approximately 35% is reflected back to the input waveguide and the rest is radiated to free space. The induced damping strength depends not only on the distance between the tip and the membrane surface but also on the tip size and on the exact lateral position of the tip in respect to the cavity structure and the strength of the optical field. A theoretical study addressing the effects of the lateral and vertical position of the tip in more detail has been presented by A. F. Koenderink et. al. [13].

In Fig. 4(b) we show the experimental measurements using an AFM in the static force mode (contact mode) to probe the cavity center. Unlike the simulations, it was difficult to control the position of the AFM tip in an intermediate state limiting the experimental measurements to the two positions where the tip is not probing the cavity (curve (1)) and where the tip is in contact with the cavity surface (curve (2)). The tip used in the experiment is shaped like a polygon based pyramid with a half-cone angle in the order of 15° to 25° and has an initial tip radius of curvature of approximately 10 nm. By scanning the photonic crystal structure the surface is measured and the cavity center slowly approached reducing consecutively the scanning area. After positioning the tip onto the center of the microcavity, the tip radius of curvature is expected to be slightly increased due to abrasion (estimated increased radius of curvature ~ 30 nm). The raw measurement data have been numerically filtered so as to remove the periodic Fabry-Pérot interference. The damping effect that has

been predicted by the three dimensional simulations can be observed in the measurements when positioning the AFM tip onto the center of the cavity. In addition, comparable to the simulations, the measurements show a similar reduction in the quality factor and a similar slight red-shift in the resonance wavelength induced by the AFM tip while damping the transmission efficiency.

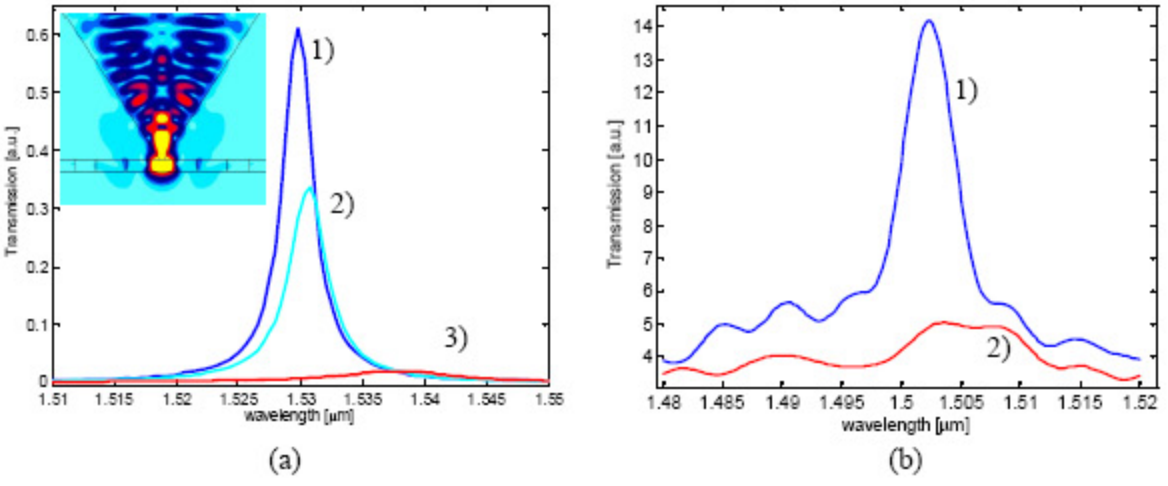

Fig. 4. (a) Simulated changes in the transmission properties of a resonant microcavity structure when probing the center of the cavity by a silicon tip. The closer the silicon tip is to the surface of the membrane (tip-surface distance: 1) 500 nm, 2) 375 nm, 3) 0 nm) the stronger is the damping effect on the transmission efficiency. The inset shows the absolute value of the calculated field distribution in the x-y plane through the center of the resonant cavity with the probing AFM tip.(b) Measured changes in the transmission properties of resonant microcavity structure when probing the center of the cavity by a silicon tip. 1) Measured transmission spectrum without the probing AFM tip. 2) Measured transmission spectrum with the AFM tip positioned on the center of the cavity using the static force mode.

When using the AFM in the dynamic force mode the cantilever with the AFM tip is vibrated near its resonance frequency with constant vibration amplitude, thus experiencing only intermittent contact with the surface. In consequence, when positioning the tip onto the center of the microcavity the damping effect is modulated and a modulation of the transmission signal is achieved. In Fig. 5, the modulated in-plane transmission signal with its frequency corresponding to the resonance frequency of the cantilever has been measured. In our case the resonance frequency is in the order of 180 kHz. The mechanically controlled modulation frequency of the optical signal depends on the resonance characteristics of the cantilever. For example, by reducing the geometry of the cantilever its resonance frequency can be increased and the optical signal could be modulated with higher speed, reaching the MHz regime.

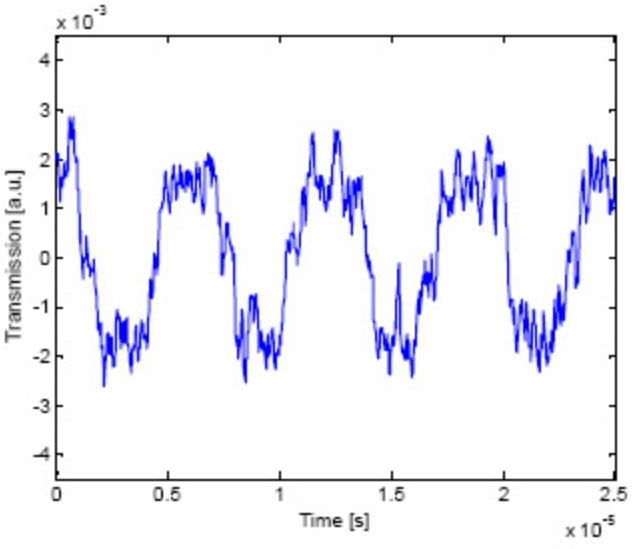

Fig. 5. Measured transmitted signal modulated at ~180 kHz by the AFM tip in the dynamic mode with the corresponding resonance frequency of the cantilever. The observed parasitic, small amplitude oscillations are most probably due to mechanical vibrations perturbing the cantilever modulation.

In a second configuration, the AFM tip is inserted into one of the Bragg mirror holes at the edge of the cavity, as indicated in Fig. 6. In our simulations we observe that as the Silicon tip enters the air hole, the resonant wavelength of the microcavity is red-shifted without significantly lowering the quality factor and the transmission efficiency (see Fig. 7(a)). At maximum insertion the calculated transmission spectrum exhibits a red shift of over 10 nm. By inserting the silicon tip the optical field confined within the microcavity sees the hole in the silicon slab being filled with silicon, which changes the effective cavity length and reduces the Bragg mirror reflectivity, thus inducing the observed shift in the resonant wavelength. In the inset of Fig. 7(a), the absolute value of the calculated field distribution illustrates how the optical field is confined within the inserted silicon tip without inducing significant vertical loss. Contrary to the first configuration where the probing silicon tip above the center of the cavity induces vertical losses, the optical field mainly remains vertically confined within the silicon membrane. Thus, tuning of the cavity becomes possible. Analog to the probing of the cavity center, we achieve a significant change in the transmission properties with a very small mechanical movement of the probing silicon tip.

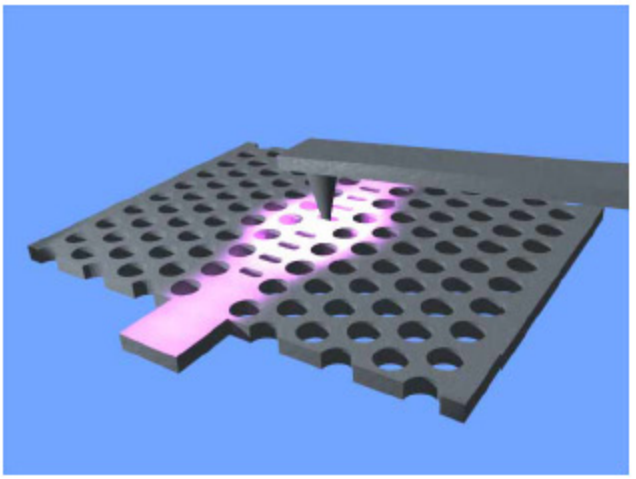

Fig. 6. Silicon AFM tip inserted into one of the holes of the Bragg mirror forming the cavity in order to induce wavelength tuning.

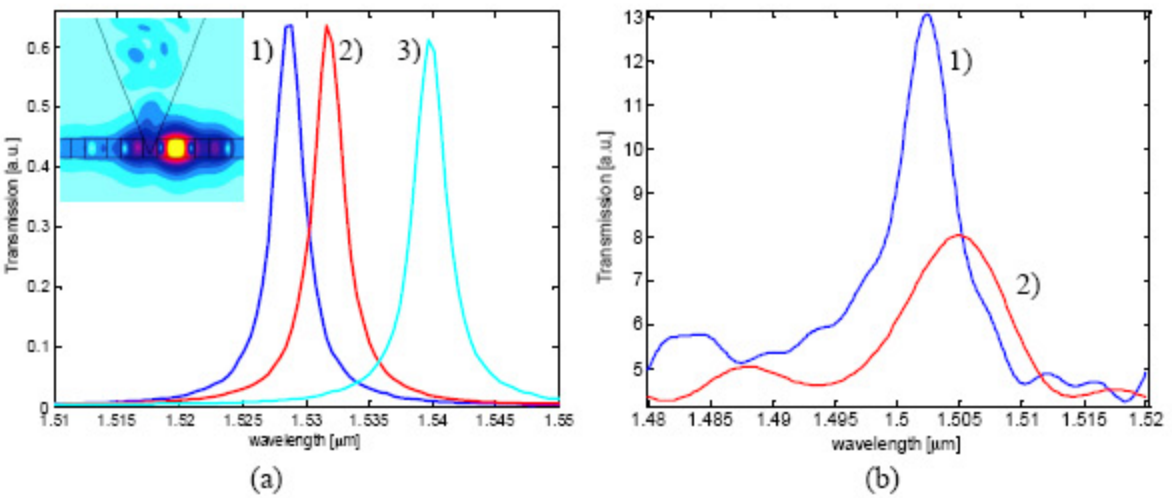

Fig. 7.(a) Simulated changes in the transmission properties of a resonant microcavity structure when inserting a silicon tip into one of the Bragg mirror holes at the etch of the cavity. The tuning strength depends on the silicon tip position (tip - membrane surface distance: 1) 0 nm, 2) -100 nm and 3) -200 nm). The inset shows the absolute value of the calculated field distribution in the x-z plane through the center of the photonic crystal waveguide with the probing AFM tip. (b) Measured changes in the transmission properties of the resonant microcavity structure when inserting a silicon tip into one of the Bragg mirror holes. 1) Measured transmission spectrum without AFM tip. 2) Measured transmission spectrum with an AFM tip inserted into one of the Bragg mirror holes using the static force mode.

Figure 7(b) shows the measured transmission spectra for the two positions where the tip is not probing the hole (curve (1)) and where the tip is inserted into a hole (curve (2)) using the AFM in the static force mode. As predicted by the three dimensional simulations we observe a slight induced red-shift, which is of the order of 2.5 nm. However, contrary to the simulations the measurements present a lowered transmission efficiency and quality factor indicating the presence of scattering losses when the AFM tip is inserted into the air hole. Small variations between the experimental and the ideal simulated configuration can cause the observed differences in the transmission properties. For example, small defects in the fabricated structure, such as variations in the hole dimensions or sidewall roughness, can

cause a different field distribution around the cavity, which may induce higher losses in the presence of the inserted AFM tip [13]. In addition, during the experiment it was difficult to determine how well the AFM tip was centered in respect to the air hole and how far the tip was inserted. The losses may also be increased due to mechanical stress in the silicon membrane induced by the probing AFM tip. Nevertheless, compared to the measurements of the first configuration the induced losses are significantly smaller, confirming the predicted tuning effect. In order to fully understand the observed results of the second configuration, we intend to carry out further tuning measurements using different types of AFM tips in the near future.

5. Conclusions

In conclusion, we have shown by simulations and first time measurements that a silicon AFM tip can be used to mechanically perturb the optical environment of a photonic crystal resonant microcavity in order to induce a change in its transmission properties. On-off switching is achieved by probing the center of the microcavity with the AFM tip, inducing vertical losses and a damping effect in the transmission efficiency. In the AFM's dynamic force mode the transmission signal has been modulated at a frequency of 180 kHz corresponding to the resonance frequency of the cantilever. By inserting the tip into one of the holes of the Bragg mirror forming the microcavity we have shown that resonant wavelength tuning becomes possible with limited losses. These results suggest a stand-alone MEMS solution to create a chip-based on-off switch or tunable filter. Furthermore, one could attempt to integrate more than one silicon tip to combine filter and tuning functionalities on one device. By separately controlling the position of the different tips a programmable integrated optical circuit with higher integration density and functionality could be achieved.

Acknowledgments

The authors would like to acknowledge S.Gautsch and U. Staufer for the fabrication of the samples by e-beam lithography in the labs of IMT-Samlab. We gratefully acknowledge R. Stanley from the Swiss Center of Electronics and Microtechnology (CSEM) for useful discussions. This work is funded under a joint projects program between the Swiss Center of Electronics and Microtechnology and the IMT-Uni Neuchâtel.